Title

Immunoproteasome inhibition and bioactivity of thiasyrbactins.

Journal

Bioorganic & medicinal chemistry, 26(2)

ISSN

0968-0896

Authors

Bakas, Nicole A
Schultz, Chad R
Yco, Lisette P
et al.

Publication Date

2018

DOI

10.1016/j.bmc.2017.11.048

Immunoproteasome Inhibition and Bioactivity of Thiasyrbactins

Nicole A. Bakas,[1] Chad R. Schultz,[2] Lisette P. Yco,[2] Christopher C. Roberts,[1] Chia-en A. Chang,[1] André S. Bachmann,,[2,4] and Michael C. Pirrung*[1,3,4]*

[1]Department of Chemistry, University of California, Riverside, CA 92521, USA.

[2]Department of Pediatrics and Human Development, College of Human Medicine, Michigan State University, Grand Rapids, MI 49503, USA.

[3]Department of Pharmaceutical Sciences, University of California, Irvine, CA 92697 *USA.*

[4]Equal contribution.

ABSTRACT

A family of macrodilactam natural products, the syrbactins, are known proteasome inhibitors. A small group of syrbactin analogs was prepared with a sulfur-for-carbon substitution to enhance synthetic accessibility and facilitate modulation of their solubility. Two of these compounds surprisingly proved to be inhibitors of the trypsin-like catalytic site, including the immunoproteasome. Their bound and free conformations suggest special properties of the thiasyrbactin ring are responsible for this unusual preference, which may be exploited to develop selective drug-like immunoproteasome inhibitors.

Keywords: proteasome; macrolactam; conformational analysis; trypsin-like site; neuroblastoma

Corresponding Authors. *Tel.: (951) 827-2722. Fax: (951) 827-2749. E-mail: Michael.pirrung@ucr.edu. *Tel.: (616) 331-5982. Fax: (616) 331-5869. E-mail: andre.bachmann@hc.msu.edu

1. Introduction

The syrbactins are a family of bacterial, macrocyclic, non-ribosomal peptide natural products active against the mammalian proteasome.[1] Their α,β-unsaturated lactam functionality reacts covalently with the catalytic Thr1 residue of proteasome catalytic subunits. Given the clinical success of the proteasome inhibitors bortezomib[2] (BTZ), ixazomib, and carfilzomib[3] against cancers such as multiple myeloma and mantle cell lymphoma,[4] intense investigations into the syrbactins followed their initial discovery.[5,6] Unlike some other proteasome inhibitors, even some used clinically, the syrbactin syringolin A is quite selective for proteasome β subunits over other protein targets, as demonstrated by affinity-based protein profiling.[7,8,9] Several syntheses of the natural syrbactins themselves have been reported, and significant work to prepare analogs has been pursued.[10-13] We recently reported the compound TIR-199 (Chart 1),[14] the first syrbactin to demonstrate activity against tumor cell lines in animal studies. It is most potent against the chymotrypsin-like activity of the β5 constitutive proteasome subunit, which can be ascribed to structural features derived from other syrbactins including the natural product glidobactin A, which was discovered through its intrinsic activity against tumor cell lines.[15] Its key structural features include the macrolactam methyl group and the long unbranched, unfunctionalized side chain. A straight-chain alkyl urea side chain similar to that of glidobactin A was originally applied to syrbactin analogs by Kaiser.[11] Maintaining this feature in the analogs from which TIR-

199 emerged enabled SAR for syrbactin macrolactam cores to be readily discerned. Pre-clinical assays of TIR-199 showed it has low aqueous solubility without co-solvents, hampering studies of bioavailability and cellular transport. Approaches to enhance the solubility of syrbactins were therefore of high priority. Both this goal and the desire for synthetic simplification from the 10-step synthesis of TIR-199 drove the study described herein.

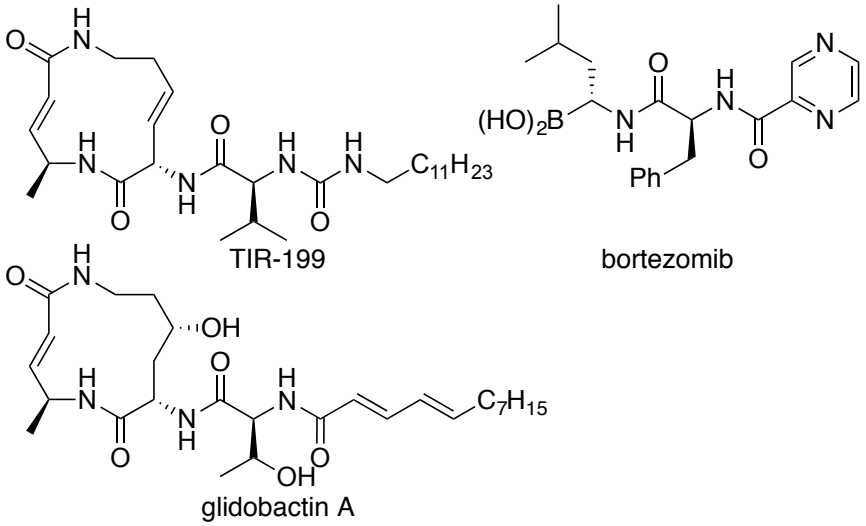

Chart 1. TIR-119, the approved drug bortezomib (Velcade®), and the natural product glidobactin A.

The design of the current family of syrbactins referred to informally as NAMs was based on our concise syringolin B analog synthesis[13] that can be applied to any lysine analog. Here it exploits the commercial compound β-aminoethylcysteine, or thialysine. Its sulfur was envisioned to provide a synthetic handle to enable late-stage strategies to enhance solubility. Its TIR-199-based macrodilactam can be accessed synthetically in only a few steps. The specific compounds prepared in this study are shown in Chart 2. Compounds **1** and **2** are inspired by TIR-199, including most of its structure but replacing the isolated alkene. The sulfoxide in **2** is at the same position as the alcohol of glidobactin A and could replicate its stereochemistry. Compounds **3**

and **4** are inspired by bortezomib, in that it is a dipeptide with an electrophilic *C*-terminus and an *N*-terminal pyrazine. The same spatial relationship between the electrophilic carbon and the pyrazine seen in bortezomib is found in the unsaturated amide of **3** and **4**. Compound **5** retains the core of **1** and **2** but adds a branched, saturated, chiral carbon in the side chain, one strategy recommended to enhance solubility.[16-18] Compound **6** likewise retains the macrolactam-valine but terminates it with the more polar pyrazinamide. All were evaluated computationally for their physicochemical properties that affect drug-likeness.[19,20] These results are summarized in Table 1.

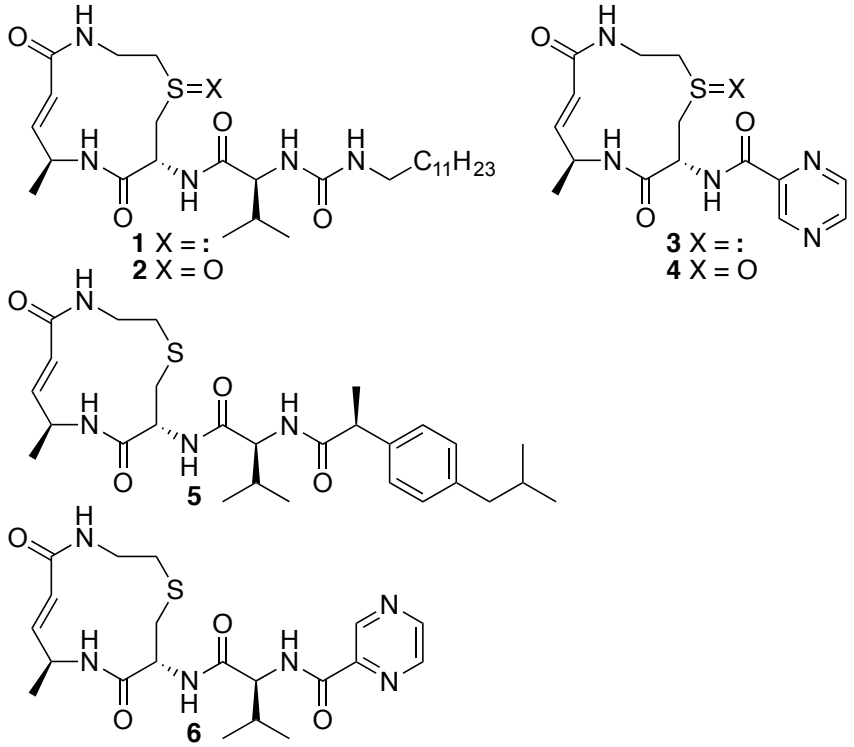

Chart 2. Synthetic syrbactin analogs prepared in this study.

Table 1. Properties affecting thiasyrbactin drug-likeness including solubility, hydrophobicity, and molecular weight.

Compound	NAM #	M_r (Da)	log P[a]	Log S[b]	Log S_w[a]
TIR-199	-	533	5.95	-4.51	-5.91
GlbA	-	520	3.12	-3.89	-4.24
1	105	553	5.51	-4.65	-5.75
2	135	569	3.89	-4.36	-4.83
3	41	349	-0.76	-3.03	-1.50
4	111	365	-2.38	-2.91	-0.58
5	93	531	3.86	-4.52	-5.09
6	95	448	-0.05	-3.56	-2.33

[a]Calculated using the method in ref. 19. [b]Calculated using the method in ref. 20.

2. Results

2.1. Synthesis

The synthesis of the core macrodilactam common to all of the targets prepared here is summarized in Scheme 1. The commercial aminoethylcysteine hydrochloride (**7**, thialysine), was converted in one pot to the ε-phosphonoacetatamide/α-Boc derivative **9** in 83% yield. Small

quantities of the doubly Boc-protected and α-phosphonoacetatamide/ε-Boc amino acids were also formed, and experimental optimization was necessary to reduce their levels. Conventional carbodiimide coupling with alaninol gave **10** in 68% yield and set the stage for macrocycle formation. Dess-Martin oxidation of **10** gave an intermediate aldehyde that was neither purified nor handled unnecessarily. We have applied the Horner-Wadsworth-Emmons condensation as modified by Helquist[21] to the preparation of dozens of macrolactam analogs in the syrbactin family. This is a highly reliable process that gives superior yields in favorable circumstances. Here, macrolactam **11** was delivered in 58% yield.

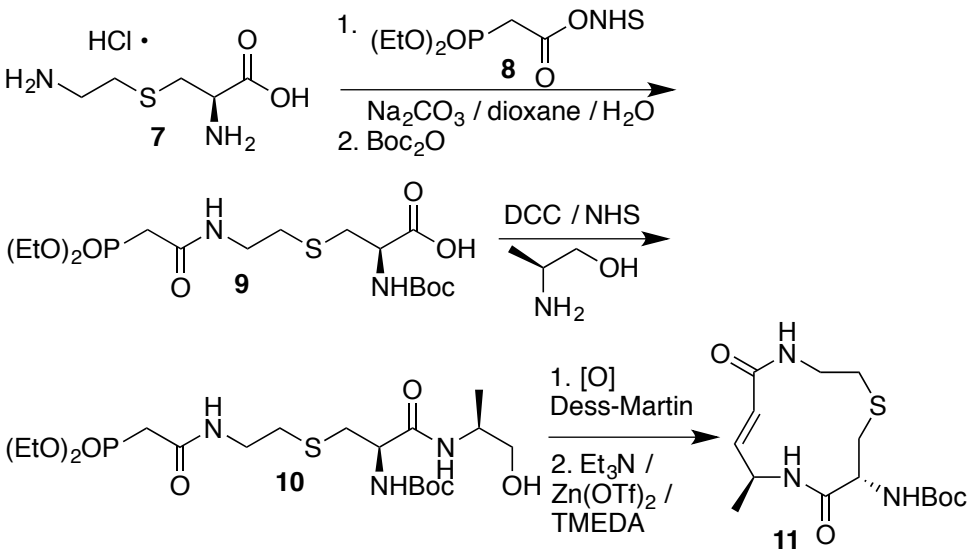

Scheme 1. Synthesis of key macrodilactam.

Stereochemical/conformational analysis of the macrolactam relied on extensive proton NMR spectra of **11**. Its C2-C3 protons form an AA'BB' system and the C11-C12 protons form an ABB' system. NMR data collected on **11** and **12** (vide infra) included high field proton, COSY and NOESY spectra. They are reported in Table 2. The three NH signals were not observed because spectra were obtained in d_4-methanol.

Table 2. NMR Data for Macrodilactams **11** and **12**

	Compound **11**				Compound **12**			
Position	δ_C[a]	δ_H[b], mult. (*J*, Hz)	COSY	NOESY	δ_C[a]	δ_H[b], mult. (*J*, Hz)	COSY	NOESY
1-S								
2	32.4	a: 2.47, m	2b, 3a, 3b	6	54.5[c]	a: 3.29, m	2b, 3a, 3b	6
		b: 2.70, ddd (5.1, 8.6, 14.0)	2a, 3a, 3b[d]			b: 2.96, ddd (7.2, 8.9, 13.9)	2a, 3a, 3b	
3	42.0	a: 3.50, m	2a, 2b, 3b	12a	37.4	a: 3.70, m	2a, 2b, 3b	12a
		b: 3.22[d], m				b: 3.48, ddd (4.5, 6.9, 16.1)	2a, 2b, 3a	12b
5	170.8				169.7			
6	121.3	6.45, d (15.7)	7	2a, 12a	120.0	6.15, d (15.4)	7, 8	2a, 12a
7	146.0	6.72, dd (4.9, 15.6)	6, 8		149.5	6.92, dd (4.8, 15.4)	6, 8	
8	48.0	4.52, m	7, 8-Me		47.9	4.57, m	6, 7, 8-Me	
8-Me	18.8	1.33, d (7.1)			18.7	1.33, d (7.1)	8	
10	172.7				170.9			
11	53.8	4.43, m	12a, 12b		52.9	4.77, t (3.5)	12a, 12b	
12	34.1	a: 3.00, dd (6.1, 14.4)	11, 12b	3a, 6	54.5[c]	a: 3.14, dd (3.8, 14.4)	11, 12b	3a, 6
		b: 3.22[d], m				b: 3.77, dd (3.2, 14.4)	11, 12a	3b
2’	157.2				157.1			
4’	81.1				81.4			
5’	28.8	1.45, s	8		28.8	1.45, s	8	

[a]Recorded at 126 MHz. [b]Recorded at 700 MHz. [c]The carbon signals 2 and 12 of compound **12** overlap. [d]The proton signals of 3b and 12b in compound **11** overlap.

We developed a conformational model of **11** to aid in understanding its chemical and biological properties and assigned the sulfoxide configuration of **12** using this data. NOESY data were used to identify proximal transannular hydrogens, which exerted substantial constraint on the available conformations. Based on molecular modeling, there are two main low-energy conformations available to **11**, with the sulfide pointing above or below the nominal plane of the ring. The macrodilactam conformation observed (Figure 1) has the sulfide below the plane and has NOE correlations between H-6 and both H-2a and H-12a. The similar coupling constants between H-11 and both H-12a and H-12b in **11** further support this conformation. If the sulfide was above the plane, the protons on carbon 12 would point down, which would cause the dihedral angles between H-11 and H-12a/12b to be closer to 135°. This would result in a larger coupling constant than is observed. Additionally, this structure would lack NOE correlations between the protons on carbons 3 and 12.

Compound **11** was oxidized to sulfoxide **12**, obtained as a single stereoisomer (Chart 3). Least hindered approach of the reagent from the equatorial direction, as commonly observed in medium rings, would yield a beta sulfinyl group. Analysis of its ^{1}H NMR spectra enabled the conformation and sulfoxide configuration to be confirmed. All adjacent protons are deshielded in the sulfinyl derivative, but the relationships among hydrogens, both in terms of dipolar and scalar couplings, are very similar to **11**, supporting a similar conformation. Table S1 compares the modeled dihedral angles and those implied from *J* couplings. Compound **12** showed additional NOE correlations between H-3b and H-12b, and H-3a and H-12a, strengthening the case for the 'sulfide below' conformation with slight inward rotation of C-3. The greatest deshielding is experienced by H-2a, which has a dihedral angle with the sulfoxide of 162°. This relationship provides the greatest downfield shift when sulfides are converted to sulfoxides.[22]

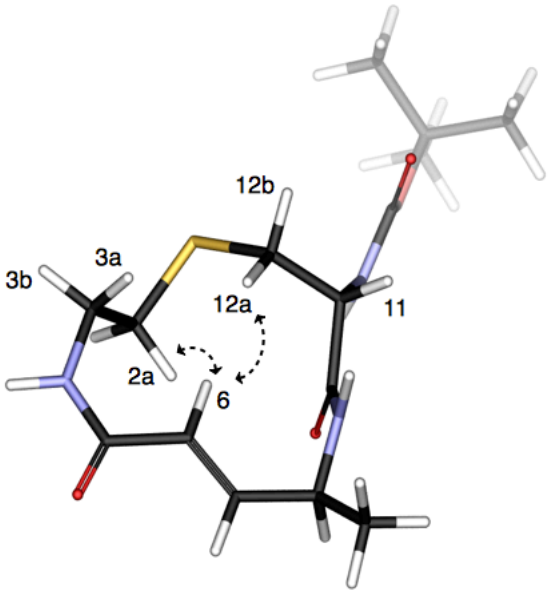

Figure 1. The conformation of macrodilactam **11** consistent with nOes and dihedral angles.[color figure]

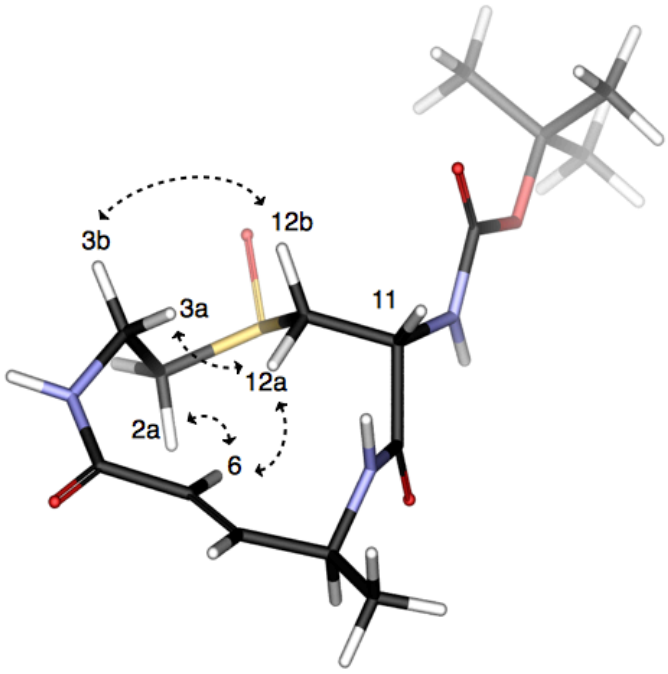

Figure 2. The conformation of macrodilactam **12** consistent with nOes and dihedral angles. [color figure]

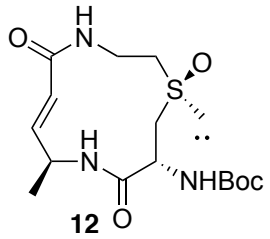

Chart 3. Thiasyrbactin sulfoxide configuration assigned to compound **12** derived from **11**.

Continuing the synthesis from **11**, the Boc group was removed with acid and the resulting hydrochloride salt was neutralized with a carbonate ion-exchange resin, in line with our past work.[13] The free base was then coupled with a valine active ester to provide **13**. Removal of its Fmoc group and urea formation with dodecyl isocyanate provided the first target **1**. Periodate oxidation yielded the sulfoxide **2** in a single stereoisomeric form, which based on spectral similarity to **12** and the precedent of its formation in the same type of reaction is assigned the beta configuration.

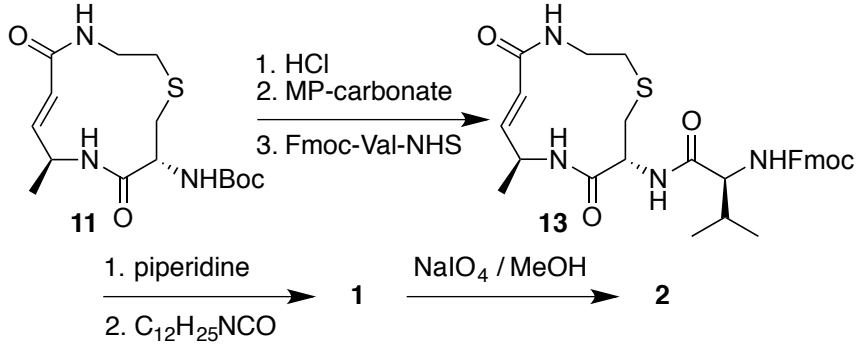

Scheme 2. Synthesis of TIR-199 analogs **1** and **2**

The other targets required active esters **14** and **15**, which were prepared conventionally from the corresponding acids.

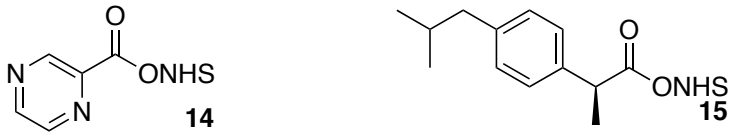

Chart 3. Side chain active esters.

Macrolactam **11** was again deprotected and converted to the free base. It was coupled with pyrazine carboxylate to yield **3** that was oxidized to yield **4** as a single stereoisomer. The ^{1}H NMR properties of **4** were very similar to those of **12**, and therefore its sulfoxide configuration was likewise assigned the beta stereochemistry. Valine-substituted macrolactam **12** was the starting point for the preparation of **5** and **6** using straightforward methods.

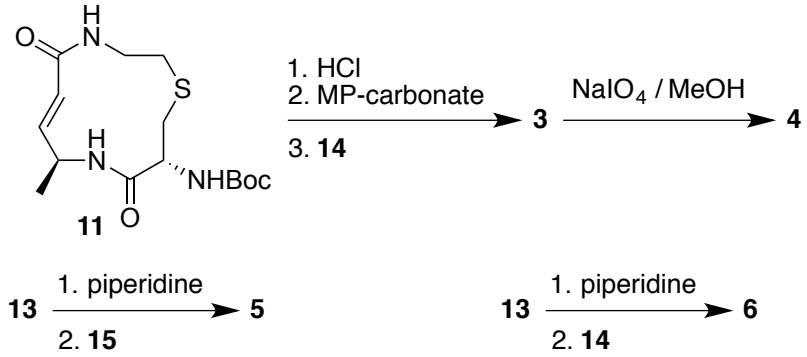

Scheme 3. Synthesis of TIR-199 analogs **3**-**6**

2.2. Biological properties

The thiasyrbactins were evaluated for their ability to inhibit each of the catalytic subunits of the constitutive and immunoproteasomes as well as for cytotoxic activity against neuroblastoma cancer cells. As **2**-**4** had no substantial activity in these assays, they will not be discussed.

To test the inhibitory activity of **1**, **5**, and **6**, we performed an *in vitro* assay and measured the three sub-catalytic activities (*i.e.*, the CT-L, C-L, and T-L activities) of the constitutive proteasome and the immunoproteasome (Table 3). For control comparison, we included the

FDA-approved peptide boronic acid proteasome inhibitor bortezomib (BTZ) and the immunoproteasome inhibitor ONX-0914 (a peptide epoxyketone related to carfilzomib) using identical experimental conditions.

While **1**, **5**, and **6** predominantly inhibit the CT-L and T-L activities of the constitutive proteasome, these compounds more potently and more selectively inhibit the T-L activity of the immunoproteasome, with no effect on the CT-L or C-L activities. It was initially surprising that inhibition of the T-L activity by **5** and **6** appears to stimulate the CT-L activity of the immunoproteasome (Figure S1). However, such behavior has been previously observed, including in actual patient samples.[23] In contrast, BTZ inhibits the CT-L and C-L sub-catalytic activities indiscriminately, with weaker activities against the T-L activity. The immunoproteasome inhibitor ONX-0914 exhibits higher potency against the immunoproteasome CT-L activity compared to the CT-L activity of the constitutive proteasome, but also inhibited the C-L and T-L activities of both proteasome types at higher concentrations. Thus, **1**, **5**, and **6** more selectively target the T-L site with Ki-50 values at 0.74, 0.75, and 1.39 μM, respectively, with no effect at ≤10 μM on the CT-L and T-L activities of the immunoproteasome. In summary, all three compounds show comparable behavior with single digit micromolar inhibition of both β2 sites in addition to the β5 site of the constitutive proteasome that was expected based on the properties of TIR-199.

Table 3. *In vitro* effects of thiasyrbactins on sub-catalytic activities of the constitutive proteasome and the immunoproteasome.

	Constitutive Proteasome		Immunoproteasome		
	Ki-50 (μM)	SD	Ki-50 (μM)	SD	
1	0.28	0.07	>10	-	CT-L (β5)
	>10	-	>10	-	C-L (β1)
	1.76	0.78	1.39	0.11	T-L (β2)
5	0.91	0.18	>10	-	CT-L (β5)
	>10	-	>10	-	C-L (β1)
	1.07	0.19	0.74	0.06	T-L (β2)
6	1.22	0.18	>10	-	CT-L (β5)
	>10	-	>10	-	C-L (β1)
	0.92	0.12	0.75	0.03	T-L (β2)
ONX-0914	0.56	0.19	0.11	0.02	CT-L (β5)
	2.07	0.30	1.32	0.21	C-L (β1)
	1.11	0.06	1.34	0.22	T-L (β2)
BTZ	0.01	0.00	0.01	0.00	CT-L (β5)
	0.02	0.00	0.03	0.01	C-L (β1)
	1.37	0.11	0.78	0.03	T-L (β2)

To study the biological effects of these thiasyrbactins, we tested their action on the viability of human neuroblastoma cells. As shown in Figure 3, **5** and **6** exhibit minimal effects on three neuroblastoma cell lines MYCN2, SK-N-Be(2)c, and SK-N-SH at the highest concentration tested (1 μM) after 24 hours exposure. In contrast, **1** significantly inhibits the viability of

MYCN2 and SK-N-SH cells at ~30-50% of control (DMSO). TIR-199 strongly inhibits viability of MYCN2 and SK-N-SH cells as previously reported[14] with little effect on SK-N-Be(2)c, a cell line originally derived from a highly metastatic, MYCN-amplified neuroblastoma tumor that exhibits chemoresistance. BTZ exhibits strong cytotoxic effects most prominently in MYCN2 and SK-N-SH cells at 0.1-1 μM.

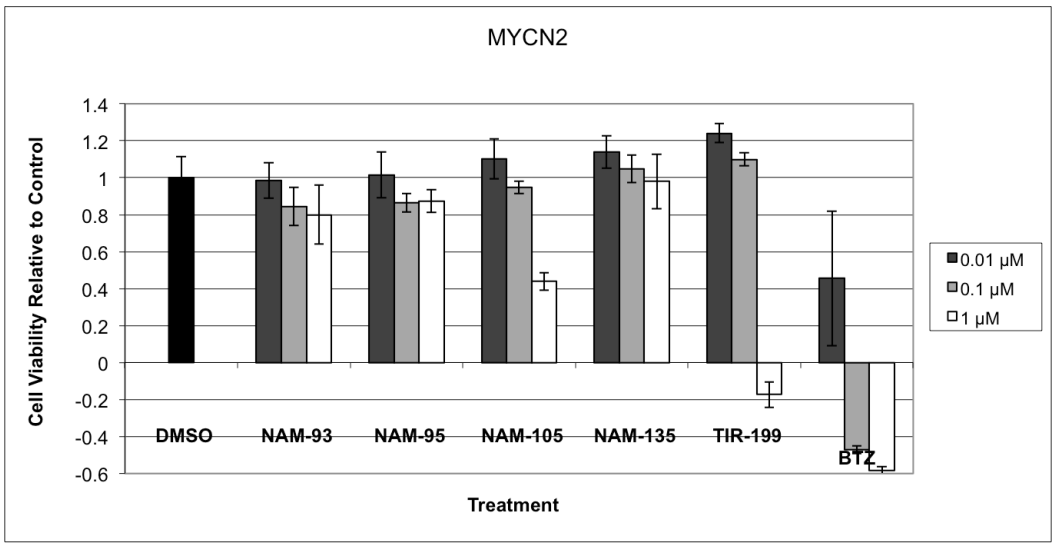
MYCN2
Cell Viability Relative to Control
1.4
1.2
1
0.8
0.6
0.4
0.2
0
-0.2
-0.4
-0.6
DMSO
NAM-93
NAM-95
NAM-105
NAM-135
TIR-199
BTZ
Treatment
0.01 μM
0.1 μM
1 μM

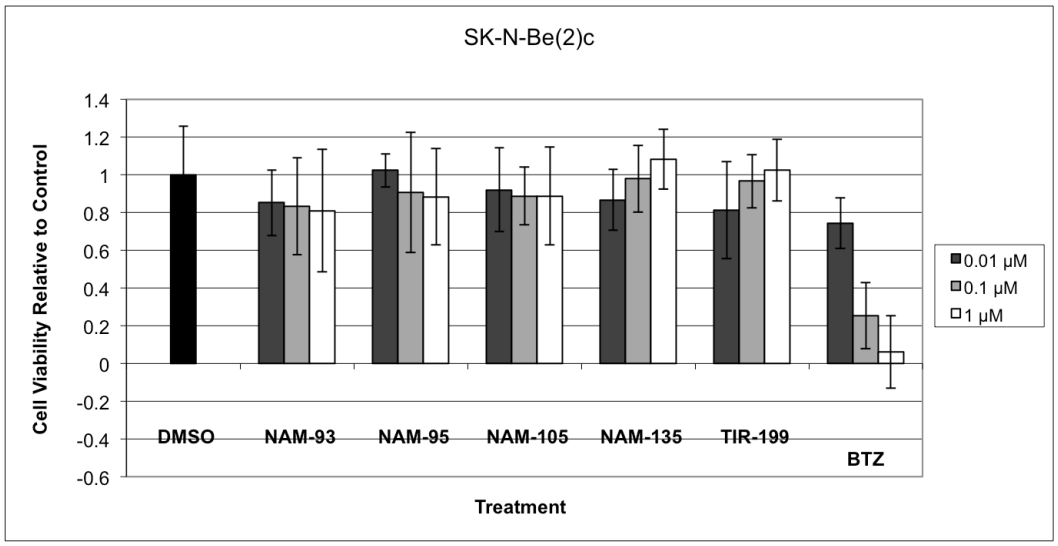
SK-N-Be(2)c
Cell Viability Relative to Control
1.4
1.2
1
0.8
0.6
0.4
0.2
0
-0.2
-0.4
-0.6
DMSO
NAM-93
NAM-95
NAM-105
NAM-135
TIR-199
BTZ
Treatment
0.01 μM
0.1 μM
1 μM

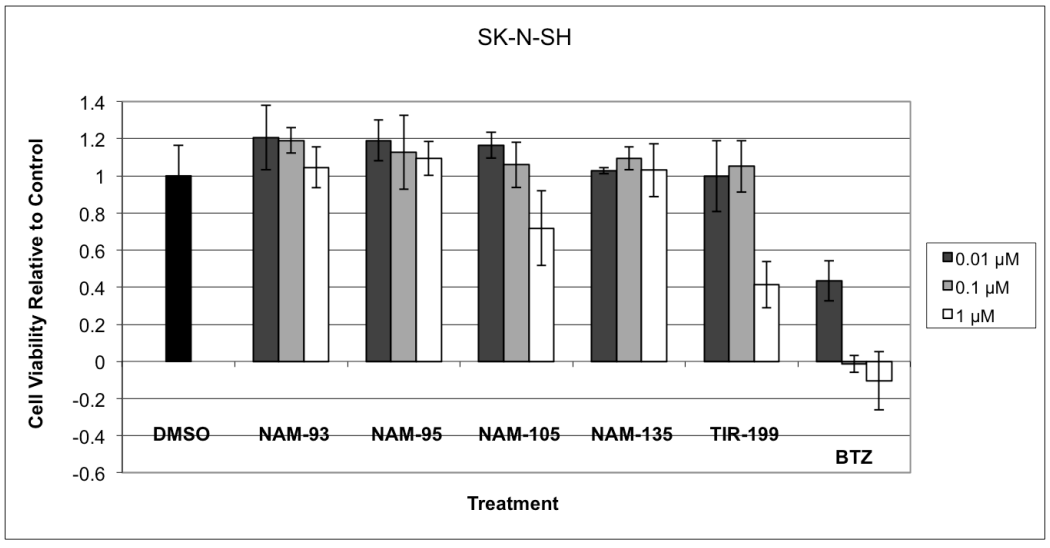
SK-N-SH
Cell Viability Relative to Control
1.4
1.2
1
0.8
0.6
0.4
0.2
0
-0.2
-0.4
-0.6
DMSO
NAM-93
NAM-95
NAM-105
NAM-135
TIR-199
BTZ
Treatment
0.01 μM
0.1 μM
1 μM

Figure 3. Effect of thiasyrbactins on the viability of human neuroblastoma cancer cells. (A) MYCN2, (B) SK-N-Be(2)c, and (C) SK-N-SH neuroblastoma cells were treated with **1**, **5**, or **6** for 24 hours at three different concentrations (0.01, 0.1, and 1 μM). Bortezomib (BTZ) was included as a control. Cell viability was measured using the MTS reagent as described in the Methods section. Data shown are representative of two independent experiments, each performed in triplicate wells (n=6).

2.3. Molecular dynamics simulation

The actions of these compounds against the trypsin-like β2 subunits were interesting, particularly of the immunoproteasome, as selective inhibition of this sub-site has been difficult to achieve. We therefore aimed to gain structural understanding of their properties via modeling. As in our earlier work,[14] binding of a thiasyrbactin to the proteasome was evaluated using molecular mechanics/generalized Born/surface area energetic post-simulation analysis of molecular dynamics trajectories. Due to significant folding of the ring, the conformation of **5** bound to the β2 site has an even more exaggerated preference for the 'sulfide below' conformation than the free compound (Figure 4). Binding of syringolin A in this site was also simulated, and it binds similar to the way it binds to the β5 site of the constitutive proteasome, with the macrolactam rather flat like in its free conformation. The conformational change is quite dramatic with **5**, resulting in several differences in the bound conformation compared to the natural product. While the C5 amide is a cis amide in both, in **5** the NH lies significantly above where it is in bound SyrA. This initiates a 3-atom excursion above the area of the corresponding ring atoms in SyrA. Whereas the N9 NH in **5** projects upward, in SyrA it projects downward. Whereas the C10 carbonyl in **5** projects downward, in SyrA it projects upward. The amide of **5** is thus 'flipped'.

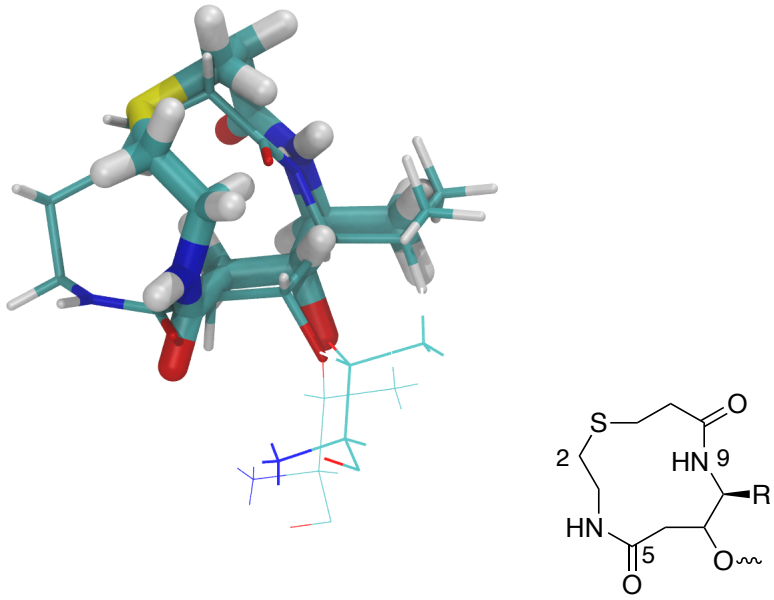

Figure 4. Comparison of the modeled macrolactam conformations of syringolin A (SyrA) and **5** bound to the β2 site of the immunoproteasome. SyrA is rendered in thin tubes and **5** in thick tubes. The Thr1 residue of the protein is shown in wire frame. The C11 side chains were removed from each molecule after modeling because they are quite different and obscure the rings. The inset shows a structural key with atom numbering. For **5**, R=Me, for SyrA R=*i*-Pr. [color figure]

Examining this conformation regarding proximal residues of the proteasome (Figure 5), the ring structure of **5** that is very different from SyrA allows the compound to rearrange itself in the binding pocket. The three-atom excursion mentioned above makes direct van der Waals contacts with side chains of Ala49, Met222, and Leu344. In these MD simulations, the N9 NH of **5** forms a stable hydrogen bond with the backbone carbonyl oxygen of Gly47 of the protein. This is the same residue that has been assigned the role of polarizing the unsaturated amide carbonyl of the syrbactins for the conjugate addition of the protein's catalytic Thr1. The C11 side chain makes

extensive non-polar protein contacts. The benzene ring of the ibuprofen is also proximal to the macrolactam that may influence the folding of this side chain against the ring.

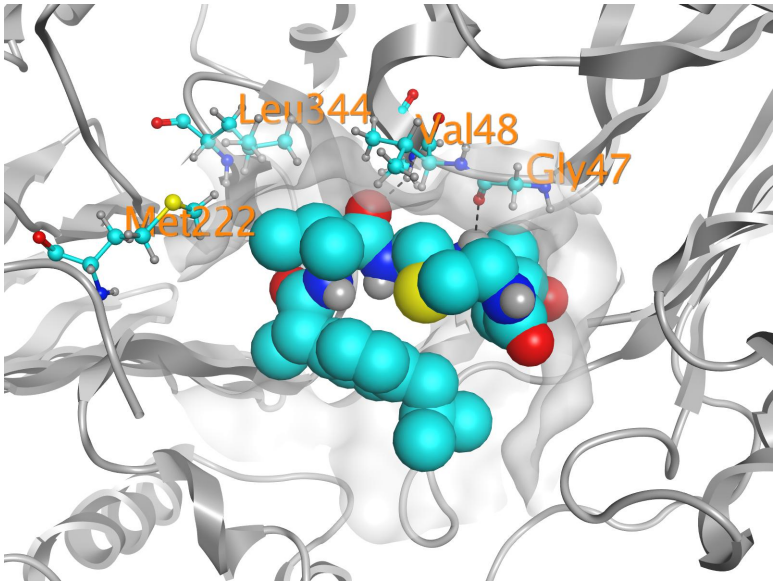

Figure 5. Modeled **5** bound to the β2 site of the immunoproteasome. The compound is rendered in Licorice, nearby protein residues are in VDW, and the remainder of the protein is in Cartoon. [color figure]

3. Discussion

The desired goals of a streamlined synthesis and enhanced solubility for syrbactin analogues were achieved in this work, though the compounds with increased solubility were not more active. Another unexpected observation was the ability of **1** and **5** to inhibit the trypsin-like β2 subunit of the immunoproteasome, whereas their parent compound, TIR-199, is a selective β5 subunit inhibitor of the constitutive proteasome. While there are several reports of selective inhibitors of the immunoproteasome trypsin-like subunit,[24-26] most are not drug-like.

Given the preference of **1** and **5** for the immunoproteasome catalytic activity that is not found in most cells, it was not very surprising that the thiasyrbactins have weak biological activity

against neuroblastoma cells. Compounds **5** and **6** are more drug-like and soluble than TIR-199, though their current potency likely limits their utility to tool compounds that can elucidate the phenotypes of selectively inhibiting the β2 subunit of the proteasome. However, epoxyketone compounds are known that have selectivity somewhat like this.[27] Even though they are not very potent on their own, they show interesting synergistic activities with other proteasome inhibitors.

An important conformational change occurs in a thiasyrbactin when bound to the β2 proteasomal subunit compared to past syrbactins. The 'flipped' C10 amide and the highly folded ring results in its contacting different protein residues.

The immunoproteasome is regarded as a next-generation target for proteasome inhibitors,[28] for both autoimmune disease[29,30] and hematologic malignancies.[31,32] The actions of the thiasyrbactins on immune cells should prove interesting, including those associated with tumor cell growth. Unlike bortezomib, syrbactins block the proteasome irreversibly and, importantly, do not inhibit normal proteases,[5] the latter of which being the main reason for the reported bortezomib-induced neuropathies in patients. The greater target selectivity of Syrbactins compared to bortezomib implies reduced off-target activity and more dose flexibility in animals models and patients.

4. Experimental Section

General. All reagents were purchased from commercial sources and were used without further purification, unless otherwise stated. Chromatographic purification of products was accomplished using flash column chromatography with silica gel 60. All melting point data were measured on a Büchi Melting Point B-545 instrument and are uncorrected. IR spectra were obtained on a Perkin Elmer Spectrum One FT-IR spectrometer or a Bruker Alpha FT-IR spectrometer using the ATR accessory and are reported in absorption frequency (cm^{-1}). The specific rotation data were measured on a Rudolph Research Analytical AutoPol IV polarimeter.

Proton (^{1}H) and carbon (^{13}C) NMR spectra were obtained on Varian Inova 300 (300 MHz and 75 MHz, respectively), Varian Inova 400 (400 MHz and 101 MHz, respectively), Varian Inova 500 (500 MHz and 126 MHz, respectively), or Bruker Avance 700 (700 MHz) spectrometers as noted, and were internally referenced to residual deuterated solvent signals and reported in terms of chemical shift (δ ppm). Mass spectra were obtained on an Agilent G3250AA LCMS instrument. Based on the criteria provided by Baell & Holloway,[33] we believe the new compounds assayed in this work have low potential for pan-assay interference and that assays to establish they do not show it were unnecessary. All tested compounds exhibited >95% purity based on clean NMR spectra without extraneous peaks.

Synthetic methods

(S)-2-(3-Dodecylureido)-3-methyl-N-((8S,11R,E)-8-methyl-5,10-dioxo-1-thia-4,9-diazacyclo dodec-6-en-11-yl)butanamide **1**. Compound **13** (19 mg, 33.6 μmol) was dissolved in 1 mL dry dimethylformamide and treated with piperidine (6 μL). The solution was stirred for 40 min and the volatiles were removed in vacuo. The reaction mixture was diluted with 1 mL dry dimethylformamide and dodecylisocyanate (16 μL, 66.4 μmol) was added. The resulting mixture was stirred at room temperature for 22 h at room temperature and concentrated in vacuo to obtain a solid that was purified by column chromatography (SiO_2, methanol/dichloromethane gradient, 0:10 to 1:9) to afford a white solid (0.0140 g, 75%). Mp: 231-233 °C. $[\alpha]^{D}_{25}$ -28.4 (*c* 0.02, MeOH). IR (neat): 3311, 3270, 3064, 2958, 2923, 2853, 1626, 1544, 1466, 1386, 1283, 1239, 1219, 1168, 1095, 1017, 961, 915, 848, 721, 643 cm^{-1}. ^{1}H NMR (400 MHz, CD_3OD): δ 6.74 (dd, J = 15.6, 4.8 Hz, 1H), 6.49 (d, J = 15.6 Hz, 1H), 4.72-4.66 (m, 1H), 4.57 – 4.47 (m, 1H), 4.10 (d, J = 5.3 Hz, 1H), 3.59 – 3.45 (m, 1H), 3.16 – 3.06 (m, 3H), 2.77 – 2.61 (m, 1H), 2.55 – 2.41 (m, 1H), 2.23 – 2.10 (m, 1H), 1.52-1.41 (m, 2H), 1.36 – 1.22 (m, 20H), 1.05 – 0.72 (m, 12H). ^{13}C

NMR (126 MHz, CD_3OD): δ 145.9, 121.5, 78.4, 71.5, 60.7, 56.4, 53.0, 48.0, 41.8, 41.1, 33.9, 33.2, 32.7, 32.0, 31.4, 30.9, 30.6, 28.1, 23.9, 20.1, 18.8, 18.0, 14.6. HRMS calcd. for $C_{28}H_{52}N_5O_4S$ $[M+H]^+$ 554.3740, found 554.3746.

(2S)-2-(3-Dodecylureido)-3-methyl-N-((8S,11R,E)-8-methyl-1-oxido-5,10-dioxo-1-thia-4,9-diazacyclododec-6-en-11-yl)butanamide **2**. Compound **1** (12.7 mg, 22.9 μmol) was dissolved in 1.5 mL of methanol and set to stir at 0 °C. Sodium periodate (5.7 mg, 26.6 μmol) was dissolved in 0.2 mL of water and added dropwise; the reaction mixture was stirred for 24 h and concentrated in vacuo. The crude solid was purified by column chromatography (SiO_2, methanol/dichloromethane gradient, 0:10 to 1:9) to give a white solid (7.8 mg, 60%). Mp: 204-206 °C. $[\alpha]^D_{25}$ -36.3 (*c* 0.024, MeOH). IR (neat): 3316, 2956, 2921, 2852, 1708, 1657, 1622, 1553, 1522, 1457, 1377, 1340, 1293, 1238, 1205, 1166, 1091, 1042, 1013, 914, 853, 815, 766, 721, 648, 580, 541, 474, 456 cm^{-1}. ^1H NMR (400 MHz, CD_3OD): δ 6.87 (dd, *J* = 15.3, 5.0 Hz, 1H), 6.16 (d, *J* = 15.5 Hz, 1H), 4.97 (t, *J* = 4.2 Hz, 1H), 4.57 – 4.33 (m, 1H), 4.08 (d, *J* = 5.4 Hz, 1H), 3.76 (dd, *J* = 14.6, 3.2 Hz, 1H), 3.71 – 3.64 (m, 1H), 3.49 – 3.42 (m, 1H), 3.17 (dd, *J* = 14.4, 4.4 Hz, 1H), 3.09 (t, *J* = 6.5 Hz, 1H), 2.97 – 2.88 (m, 1H), 2.19 – 2.12 (m, 1H), 1.47 – 1.42 (m, 2H), 1.39 – 1.12 (m, 22H), 1.06 – 0.73 (m, 12H). ^{13}C NMR (126 MHz, CD_3OD): δ 149.0, 120.2, 78.4, 60.6, 54.3, 54.1, 51.5, 47.9, 41.1, 37.2, 33.2, 32.0, 31.4, 30.9, 30.6, 28.1, 23.9, 20.1, 18.7, 18.0, 14.6. HRMS calcd. for $C_{28}H_{52}N_5O_5S$ $[M+H]^+$ 570.3689, found 570.3703.

N-((8S,11R,E)-8-Methyl-5,10-dioxo-1-thia-4,9-diazacyclododec-6-en-11-yl)pyrazine-2-carboxamide **3**. The macrolactam **11** (60.1 mg, 0.175 mmol) was treated with hydrochloric acid in ethyl acetate (3 N, 2.0 mL) and stirred for 30 min at room temperature, then concentrated in vacuo. The resulting white solid hydrochloride salt was dissolved in 2 mL dimethylformamide and MP-carbonate resin (2.94 mmol/g, 0.1801 g, 0.529 mmol) was added at 0 °C, followed by

pyrazine carboxylic acid *N*-hydroxysuccinimide ester (**14**) (49.0 mg, 0.222 mmol). The resulting mixture was stirred at 0 °C for 15 min and 14 h at room temperature and concentrated in vacuo to obtain a solid that was purified by column chromatography (SiO_2, methanol/dichloromethane gradient, 0:10 to 1:9) to give a white solid (0.0293 g, 48%). Mp: 256-258 °C. $[\alpha]^{D}_{25}$ - 13.9 (*c* 0.13, MeOH). IR (neat): 3450, 3387, 3374, 3265, 3044, 2986, 2932, 2918, 1721, 1684, 1666, 1651, 1628, 1582, 1543, 1514, 1464, 1454, 1404, 1364, 1350, 1335, 1308, 1293, 1268, 1241, 1218, 1167, 1156, 1094, 1047, 1021, 964, 947, 907, 893, 875, 852, 843, 795, 778, 734, 716, 688, 669 cm^{-1}. ^{1}H NMR (300 MHz, CD_3OD): δ 9.25 (d, *J* = 1.4 Hz, 1H), 8.82 (d, *J* = 2.5 Hz, 1H), 8.71 (dd, *J* = 2.4, 1.5 Hz, 1H), 6.77 (dd, *J* = 15.6, 4.9 Hz, 1H), 6.49 (d, *J* = 15.7 Hz, 1H), 4.95 (dd, *J* = 5.8, 1.9 Hz, 1H), 4.61 – 4.49 (m, 1H), 3.58 (ddd, *J* = 14.7, 8.8, 4.1 Hz, 1H), 3.35 (d, *J* = 2.8 Hz, 1H), 3.28 – 3.17 (m, 2H), 2.77 (ddd, *J* = 14.4, 9.0, 5.1 Hz, 1H), 2.48 (ddd, *J* = 14.9, 9.1, 6.0 Hz, 1H), 1.37 (d, *J* = 7.1 Hz, 3H). ^{13}C NMR (126 MHz, CD_3OD): δ 171.7, 170.7, 164.3, 149.2, 146.0, 145.7, 145.1, 144.8, 121.2, 52.5, 48.1, 42.0, 33.7, 32.0, 18.8. HRMS calcd. for $C_{15}H_{20}N_5O_3S$ $[M+H]^+$ 350.1287, found 350.1298.

N-((8S,11R,E)-8-Methyl-1-oxido-5,10-dioxo-1-thia-4,9-diazacyclododec-6-en-11-yl)pyrazine-2-carboxamide **4**. Compound **3** (6.2 mg, 17.7 μmol) was dissolved in 1 mL of methanol and set to stir at 0 °C. Sodium periodate (4.3 mg, 20.1 μmol) was dissolved in 0.1 mL of water and added drop-wise, and the reaction mixture was stirred for 24 hours and concentrated in vacuo. The white crude solid was purified by column chromatography (SiO_2, methanol/dichloromethane gradient, 0:10 to 1:9) to give a white solid (6.4 mg, 98%). Mp: 250-252 °C. $[\alpha]^{D}_{25}$ -32.0 (*c* 0.05, MeOH). IR (neat): 3370, 3332, 3267, 3067, 2956, 2922, 2852, 1674, 1661, 1646, 1629, 1583, 1529, 1472, 1454, 1407, 1366, 1354, 1282, 1267, 1238, 1213, 1169, 1155, 1091, 1050, 1021, 1006, 971, 945, 908, 883, 852, 775, 734, 717, 677, 631, 582, 553, 463, 432 cm^{-1}. ^{1}H NMR (400

MHz, d_6-DMSO): δ 9.21 (s, 1H), 8.91 (d, *J* = 2.1 Hz, 1H), 8.75 (d, *J* = 7.5 Hz, 1H), 6.83 (dd, *J* = 15.3, 4.6 Hz, 1H), 6.06 (d, *J* = 15.0 Hz, 1H), 5.16 (dd, *J* = 7.5, 3.6 Hz, 1H), 4.51 (dd, *J* = 12.6, 7.3 Hz, 1H), 4.04 – 3.95 (m, 1H), 3.55 – 3.45 (m, 1H), 3.25 – 3.14 (m, 3H), 2.75 – 2.65 (m, 1H), 1.24 (d, *J* = 6.4 Hz, 3H). ^{13}C NMR (126 MHz, d_6-DMSO): δ 168.0, 165.5, 162.0, 148.2, 147.5, 143.7, 143.5, 143.3, 118.5, 55.3, 52.9, 50.5, 45.8, 36.5, 18.5. HRMS calcd. for $C_{15}H_{19}N_5O_4SNa$ $[M+Na]^+$ 388.1055, found 388.1040.

(S)-2-((S)-2-(4-Isobutylphenyl)propanamido)-3-methyl-N-((8S,11R,E)-8-methyl-5,10-dioxo-1-thia-4,9-diazacyclododec-6-en-11-yl)butanamide **5**. Compound **13** (22.2 mg, 39.3 μmol) was dissolved in 1 mL dry dimethylformamide and treated with piperidine (10 μL) and the solution was stirred for 30 min and volatiles were removed in vacuo. The residue was dissolved in 1 mL dimethylformamide and (*S*)-(+)-ibuprofen *N*-hydroxysuccinimide ester (**15**) (27.8 mg, 91.6 μmol) was added. The resulting mixture was stirred at 0 °C for 30 min and 24 h at room temperature and concentrated in vacuo to obtain a white solid that was purified by column chromatography (SiO_2, methanol/dichloromethane gradient, 0:10 to 1:9) to give a white solid (15.2 mg, 73%). Mp: 189-191 °C. $[\alpha]^D_{25}$ -37.1 (*c* 0.07, MeOH). IR (neat): 3274, 3055, 2957, 2925, 2870, 1706, 1630, 1535, 1459, 1382, 1282, 1220, 1166, 1088, 1030, 908, 848, 815, 777, 718, 659, 639, 577, 459 cm^{-1}. ^{1}H NMR (300 MHz, CD_3OD): δ 7.25 (d, J = 8.1 Hz, 2H), 7.08 (d, J = 7.9 Hz, 2H), 6.72 (dd, J = 15.7, 4.9 Hz, 1H), 6.46 (d, J = 15.4 Hz, 1H), 4.60 (dd, J = 6.1, 1.9 Hz, 1H), 4.54 – 4.45 (m, 1H), 4.21 (d, J = 7.4 Hz, 1H), 4.19 – 4.11 (m, 1H), 3.75 (dd, J = 14.4, 7.2 Hz, 1H), 3.55 – 3.42 (m, 1H), 3.26 – 3.16 (m, 1H), 3.12 (dd, J = 14.5, 2.2 Hz, 1H), 2.95 (dd, J = 14.5, 6.2 Hz, 1H), 2.44 (d, J = 7.1 Hz, 2H), 2.41 – 2.33 (m, 1H), 2.12 – 2.03 (m, 1H), 1.88 – 1.78 (m, 1H), 1.46 (d, J = 7.1 Hz, 3H), 1.37 – 1.27 (m, 6H), 0.97 – 0.88 (m, 9H). ^{13}C NMR (126 MHz, CD_3OD): δ 177.7, 176.0, 173.1, 171.6, 170.9, 145.9, 141.6, 139.9, 130.5, 128.5, 121.5,

60.4, 53.1, 48.0, 47.0, 46.2, 42.0, 33.7, 32.7, 31.8, 31.6, 30.8, 30.1, 28.6, 26.4, 22.9, 19.9, 19.0, 18.8. HRMS calcd. for $C_{28}H_{42}N_4O_4SNa$ $[M+Na]^+$ 553.2825, found 553.2802.

N-((S)-3-Methyl-1-(((8S,11R,E)-8-methyl-5,10-dioxo-1-thia-4,9-diazacyclododec-6-en-11-yl) amino)-1-oxobutan-2-yl)pyrazine-2-carboxamide **6**. Compound **13** (59.7 mg, 0.106 mmol) was dissolved in 2 mL dry dimethylformamide and treated with piperidine (20 μL). The solution was stirred for 30 min and the volatiles were removed in vacuo. The residue was dissolved in 2 mL dimethylformamide and pyrazine carboxylic acid *N*-hydroxysuccinimide ester (**14**) (48.0 mg, 0.217 mmol) was added. The resulting mixture was stirred for 20 h at room temperature and concentrated in vacuo to obtain a solid that was purified by column chromatography (SiO_2, methanol/dichloromethane gradient, 0:10 to 1:9) to give a white solid (19.8 mg, 42%). Mp: 241-243 °C. $[\alpha]^D_{25}$ -35.2 (*c* 0.05, MeOH). IR (neat): 3289, 3273, 3058, 2962, 2929, 2874, 1634, 1513, 1450, 1389, 1336, 1291, 1218, 1164, 1095, 1047, 1019, 961, 889, 859, 847, 775, 731, 645, 577, 439 cm^{-1}. ^1H NMR (400 MHz, CD_3OD): δ 9.24 (d, J = 1.1 Hz, 1H), 8.81 (d, J = 2.4 Hz, 1H), 8.71 (dd, J = 2.3, 1.5 Hz, 1H), 6.72 (dd, J = 15.6, 4.8 Hz, 2H), 6.49 (d, J = 15.6 Hz, 1H), 4.71 (dd, J = 19.0, 4.1 Hz, 1H), 4.59 – 4.55 (m, 1H), 4.51 (dd, J = 13.9, 7.5 Hz, 1H), 3.55 – 3.46 (m, 1H), 3.27 – 3.16 (m, 2H), 3.05 (dd, J = 14.3, 6.4 Hz, 2H), 2.73 – 2.65 (m, 1H), 2.54 – 2.45 (m, 1H), 2.30 – 2.18 (m, 1H), 1.33 (d, J = 7.1 Hz, 3H), 1.05 – 0.99, m, 6H). ^{13}C NMR (101 MHz, CD_3OD): δ 173.7, 172.7, 171.7, 170.9, 165.1, 149.0, 145.9, 145.0, 121.5, 60.5, 59.9, 53.3, 53.1, 48.0, 41.9, 33.9, 32.8, 31.8, 29.7, 20.1, 19.9, 18.8. HRMS calcd. for $C_{20}H_{28}N_6O_4SNa$ $[M+Na]^+$ 471.1790, found 471.1796.

tert-*Butyl ((S)-3-((2-(2-(diethoxyphosphoryl)acetamido)ethyl)thio)-1-(((S)-1-hydroxypropan-2-yl)amino)-1-oxopropan-2-yl)carbamate* **10.** L-4-Thialysine hydrochloride salt (**7**) (0.2965 g, 1.48 mmol) was dissolved in dioxane/water (1:1, 4 mL) and cooled to 0 °C. Sodium carbonate

(0.3149 g, 2.97 mmol) was added to the mixture at 0 °C. After 30 min, phosphonoacetic acid *N*-hydroxysuccinimide ester (**8)** (0.4352 g, 1.48 mmol) was added and the mixture was stirred for 1 h at 0 °C and for 5 days at room temperature. Boc anhydride (0.6058 g, 2.78 mmol) dissolved in a minimum amount of dioxane was added drop-wise to the reaction mixture, which was stirred for 20 h at room temperature. The reaction mixture was washed with ethyl acetate (10 mL) to remove organic impurities. The aqueous phase was acidified to pH 2 using 1N hydrochloric acid, and extracted with ethyl acetate (4 × 15 mL). The combined organic extract was dried over anhydrous magnesium sulfate and concentrated to afford **9** as a colorless oil. This compound was used in the subsequent step without further purification.

The crude material **9** (0.5112 g, 1.16 mmol) was dissolved in 11 mL dry dichloromethane and set to stir at 0 °C. *N*,*N*'-Dicyclohexylcarbodiimide (0.2904 g, 1.41 mmol) and *N*-hydroxysuccinimide (0.1347 g, 1.17 mmol) were added at 0 °C, followed by L-alaninol (0.18 mL, 2.31 mmol). The mixture was stirred at 0 °C for 30 min, then for 20 h at room temperature and the *N*,*N*'-dicyclohexylurea was filtered off. The filtrate was concentrated to afford a yellowish oil that was purified by column chromatography (SiO_2, acetone/dichloromethane gradient, 1:4 to 4:1) to afford the title compound **10** as a colorless oil (0.3987 g, 54%). $[\alpha]^{D}_{25}$ -14.99 (*c* 1.0, MeOH). IR (neat): 3289, 3282, 2978, 2931, 2875, 1711, 1651, 1531, 1454, 1411, 1392, 1365, 1239, 1164, 1097, 1048, 1020, 968, 865, 839, 781 cm^{-1}. ^{1}H NMR (300 MHz, $CDCl_3$): δ 7.81 (s, 1H), 7.57 (d, *J* = 5.7 Hz, 1H), 5.59 (d, *J* = 8.4 Hz, 1H), 4.37 – 4.24 (m, 1H), 4.20 – 4.07 (m, 4H), 4.05 – 3.96 (m, 1H), 3.66 (dd, *J* = 11.4, 3.4 Hz, 2H), 3.48 (dd, *J* = 11.1, 5.8 Hz, 1H), 3.27 (br s, 1H), 2.90 – 2.78 (m, 4H), 2.67 – 2.54 (m, 1H), 1.42 (s, 9H), 1.32 (q, *J* = 7.0 Hz, 6H), 1.16 (d, *J* = 6.8 Hz, 3H)**.** ^{13}C NMR (75 MHz, $CDCl_3$): δ 170.7, 164.6, 155.9, 80.1, 66.1,

63.1, 62.9, 54.6, 47.9, 39.7, 36.7, 36.0, 34.3, 33.7, 28.4, 16.8, 16.5. HRMS calcd. for $C_{19}H_{39}N_3O_8PS$ $[M+H]^+$ 500.2195, found 500.2208.

tert-*Butyl ((8S,11R,E)-8-methyl-5,10-dioxo-1-thia-4,9-diazacyclododec-6-en-11-yl) carbamate* **11**. Dess-Martin periodinane (0.4123 g, 0.972 mmol) was added to a stirring solution of phosphono-alcohol **10** (0.4051 g, 0.811 mmol) in 8 mL of dry dichloromethane at room temperature and stirred for 45 min. The reaction mixture was diluted with 12 mL dichloromethane and 24 mL of a 1:1 mixture of sat $NaHCO_3$ and 2% sodium thiosulfate was added. The mixture was stirred vigorously until the organic phase became clear, then the phases were separated. The organic phase was dried over sodium sulfate, filtered, and concentrated in vacuo without warming to obtain an aldehyde that was used without purification in the subsequent step.

Tetramethylethylenediamine (0.15 mL, 1.00 mmol) and triethylamine (0.46 mL, 3.30 mmol) were added to a stirring suspension of zinc triflate (0.6566 g, 1.81 mmol) in 120 mL dry tetrahydrofuran at room temperature, and stirred for 45 minutes under an inert atmosphere. The crude phosphono-aldehyde was dissolved in 70 mL dry tetrahydrofuran and added drop-wise to the suspension over 2.5 h. The reaction mixture was stirred at room temperature for 21 h and concentrated in vacuo to ca. 10 mL. The residue was diluted with 100 mL ethyl acetate and washed with 50 mL each of brine and 1% hydrochloric acid. The organic phase was dried over magnesium sulfate and concentrated to afford a yellowish oil that was purified by chromatography (SiO_2, acetone/dichloromethane gradient, 1:4 to 4:1) to afford the title compound as a white solid film (0.1624 g, 58%). Mp: 176-179 °C. $[\alpha]^D_{25}$ -55.38 (*c* 0.30, MeOH). IR (neat): 3308, 2978, 2933, 1706, 1663, 1635, 1494, 1455, 1393, 1367, 1247, 1225, 1159, 1095, 1057, 1030, 974, 913, 885, 848, 759, 737 cm^{-1}. ^1H NMR (700 MHz, CD_3OD): δ 6.72 (dd, *J* =

15.6, 4.9 Hz, 1H), 6.45 (d, *J* = 15.6 Hz, 1H), 4.54 – 4.48 (m, 1H), 4.43 (d, *J* = 4.4 Hz, 1H), 3.54 – 3.46 (m, 2H), 3.26 – 3.18 (m, 2H), 3.00 (dd, J = 14.4, 6.1 Hz, 1H), 2.70 (ddd, J = 14.0, 8.6, 5.8 Hz, 1H), 2.51 – 2.43 (m, 1H), 1.45 (s, 9H), 1.33 (d, *J* = 7.1 Hz, 3H). ^{13}C NMR (101 MHz, CD_3OD): δ 172.7, 170.8, 157.2, 146.0, 121.3, 81.1, 53.8, 48.0, 42.0, 34.1, 32.4, 28.8, 18.8. HRMS calcd. for $C_{15}H_{26}N_3O_4S$ $[M+H]^+$ 344.1644, found 344.1650.

tert-*Butyl ((8S,11R,E)-8-methyl-1-oxido-5,10-dioxo-1-thia-4,9-diazacyclododec-6-en-11-yl) carbamate* **12**. The macrolactam **11** (10.5 mg, 30.6 μmol) was dissolved in 1 mL of methanol and set to stir at 0 °C. Sodium periodate (8.2 mg, 38.3 μmol) was dissolved in 0.1 mL of water and added drop-wise, and the reaction mixture was stirred for 24 hours and concentrated in vacuo. The white crude solid was purified by column chromatography (SiO_2, 1:9 methanol/dichloromethane) to give a white solid (9.8 mg, 89%). Mp: decomposition at 210 °C. $[\alpha]^D_{25}$ -108.76 (*c* 0.3, MeOH). IR (neat): 3417, 3295, 3218, 3094, 2975, 2927, 2467, 2387, 2263, 2204, 1710, 1671, 1632, 1535, 1469, 1366, 1249, 1162, 1018, 986, 852, 789, 668, 637, 569, 514, 432 cm^{-1}. ^{1}H NMR (700 MHz, CD_3OD): δ 6.92 (dd, J = 15.4, 4.8 Hz, 1H), 6.15 (d, J = 15.4 Hz, 1H), 4.77 (t, J = 3.5 Hz, 1H), 4.59 – 4.55 (m, 1H), 3.77 (dd, J = 14.4, 3.2 Hz, 1H), 3.73 – 3.67 (m, 1H), 3.48 (ddd, J = 16.1, 6.9, 4.5 Hz, 1H), 3.30 – 3.27 (m, 1H), 3.14 (dd, J = 14.4, 3.8 Hz, 1H), 2.96 (ddd, J = 13.9, 8.9, 7.2 Hz, 1H), 1.45 (s, 9H), 1.33 (d, J = 7.1 Hz, 3H). ^{13}C NMR (126 MHz, CD_3OD): δ 171.0, 169.7, 157.1, 149.5, 120.0, 81.4, 54.5, 54.4, 52.9, 47.9, 37.4, 28.8, 18.7. HRMS calcd. for $C_{15}H_{26}N_3O_5S$ $[M+H]^+$ 360.1588, found 360.1596.

(9H-Fluoren-9-yl)methyl ((S)-3-methyl-1-(((8S,11R,E)-8-methyl-5,10-dioxo-1-thia-4,9-diaza cyclododec-6-en-11-yl)amino)-1-oxobutan-2-yl)carbamate **13**. The macrolactam **11** (0.1231 g, 0.358 mmol) was treated with hydrochloric acid in ethyl acetate (3N, 3.0 mL) and stirred for 30 min at room temperature, then concentrated in vacuo. The resulting white solid hydrochloride

salt was dissolved in 4 mL dry dimethylformamide and set to stir at 0 °C. MP-Carbonate resin (2.94 mmol/g, 0.3663 g, 1.08 mmol) was added, followed by *N*-Fmoc-L-valine *N*-hydroxysuccinimide ester (0.1952 g, 0.447 mmol). The reaction mixture was stirred for 30 min at 0 °C, then 24 h at room temperature. The reaction mixture was concentrated in vacuo to obtain a white solid that was purified by column chromatography (SiO_2, methanol/dichloromethane gradient, 0:10 to 1:9) to afford a white solid (0.1217 g, 60%). Mp: 207-209 °C. $[\alpha]^{D}_{25}$ -55.43 (*c* 0.05, MeOH). IR (neat): 3282, 3063, 2959, 2925, 2872, 2854, 2463, 2409, 2375, 2353, 2338, 1692, 1635, 1538, 1450, 1390, 1342, 1290, 1249, 1237, 1219, 1163, 1135, 1101, 1084, 1033, 992, 960, 852, 795, 758, 739, 730, 668 cm^{-1}. ^{1}H NMR (400 MHz, CD_3OD): δ 7.80 (d, J = 7.5 Hz, 2H), 7.71 – 7.64 (m, 2H), 7.39 (t, J = 7.4 Hz, 2H), 7.31 (t, J = 7.3 Hz, 2H), 6.72 (dd, J = 15.6, 4.9 Hz, 1H), 6.47 (d, J = 15.8 Hz, 1H), 4.71 (d, J = 5.1 Hz, 1H), 4.54 – 4.47 (m, 1H), 4.37 (t, J = 7.1 Hz, 1H), 4.25 (t, J = 6.8 Hz, 1H), 3.99 (d, J = 6.7 Hz, 1H), 3.55 – 3.46 (m, 1H), 3.20 (d, J = 14.9 Hz, 1H), 3.07 (dd, J = 14.3, 6.1 Hz, 1H), 2.73 – 2.62 (m, 1H), 2.52 – 2.42 (m, 1H), 2.19 – 2.06 (m, 1H), 1.32 (d, J = 7.0 Hz, 3H), 0.97 – 0.93 (m, 6H). ^{13}C NMR (126 MHz, CD_3OD): δ 146.0, 128.9, 128.4, 126.4, 121.1, 68.2, 62.0, 53.0, 48.0, 41.8, 33.8, 32.7, 31.8, 30.9, 19.9, 18.8. (Partial ^{13}C NMR data due to lack of compound solubility.) HRMS calcd. for $C_{30}H_{37}N_4O_5S$ $[M+H]^+$ 565.2485, found 565.2497.

General procedure for synthesizing NHS esters. The *N*-hydroxysuccinimide esters of pyrazinecarboxylic acid and (*S*)-(+)-ibuprofen were prepared by dissolving the starting acid (0.200 g, 1.0 equiv) in dry tetrahydrofuran and setting to stir at 0 °C. *N*-Hydroxysuccinimide (1.0 equiv) was added followed by *N*,*N*'-dicyclohexylcarbodiimide (1.0 equiv). The mixture was warmed to room temperature and stirred for 24 h. The *N*,*N*'-dicyclohexylurea was removed by

filtration and the filtrate was concentrated to afford a solid that was purified by column chromatography.

2,5-Dioxopyrrolidin-1-yl pyrazine-2-carboxylate **14**. A crude white solid was purified by column chromatography (SiO_2, acetone/dichloromethane, 1:4) to give a white solid (0.2757 g, 77%). Mp: 161 – 164 °C. ^{1}H NMR (300 MHz, $CDCl_3$): δ 9.40 (d, *J* = 1.4 Hz, 1H), 8.90 (d, *J* = 2.3 Hz, 1H), 8.83 (dd, *J* = 2.4, 1.5 Hz, 1H), 2.95 (s, 4H). ^{13}C NMR (101 MHz, $CDCl_3$): δ 168.9, 159.6, 149.3, 147.1, 145.2, 140.2, 25.8. IR (neat): 3501, 3324, 3276, 3078, 2929, 2851, 1875, 1806, 1785, 1703, 1653, 1626, 1571, 1533, 1468, 1449, 1420, 1399, 1360, 1306, 1260, 1243, 1203, 1183, 1153, 1075, 1060, 1048, 1025, 1011, 995, 951, 892, 876, 853, 811, 782, 764, 713 cm^{-1}. HRMS calcd. for $C_9H_8N_3O_4$ $[M+H]^+$ 222.0509, found 222.0502.

2,5-Dioxopyrrolidin-1-yl (S)-2-(4-isobutylphenyl)propanoate **15**. A crude white solid was purified by column chromatography (SiO_2, ethyl acetate/hexane gradient, 1:4 to 2:3) to give a white solid (0.2742 g, 93%). Mp: 74-76 °C. $[\alpha]^D_{25}$ 60.2 (*c* 1.0, MeOH). ^{1}H NMR (500 MHz, $CDCl_3$): δ 7.27 (d, *J* = 8.0 Hz, 2H), 7.15 (d, *J* = 7.9 Hz, 2H), 4.04 (q, *J* = 7.2 Hz, 1H), 2.79 (s, 4H), 2.47 (d, *J* = 7.2 Hz, 2H), 1.87 (dp, *J* = 13.4, 6.7 Hz, 1H), 1.64 (d, *J* = 7.2 Hz, 3H), 0.91 (d, *J* = 6.6 Hz, 6H). ^{13}C NMR (126 MHz, $CDCl_3$) δ 170.2, 169.2, 141.4, 135.6, 129.9, 129.7, 127.5, 127.3, 45.2, 42.8, 42.7, 30.3, 25.8, 22.6, 19.2, 19.1. IR (neat): 3054, 2959, 2904, 2851, 1862, 1839, 1800, 1765, 1741, 1631, 1513, 1446, 1432, 1380, 1363, 1342, 1313, 1261, 1238, 1207, 1182, 1144, 1088, 1047, 991, 962, 924, 871, 850, 814, 769, 728, 688, 669, 641, 560, 507, 464 cm^{-1}. HRMS calcd. for $C_{17}H_{21}NO_4Na$ $[M+Na]^+$ 326.1368, found 326.1368.

Biological methods

In Vitro Proteasome Activity Assay. To determine the anti-proteasome activity of the thiasyrbactins in the *in vitro* environment, we measured the three catalytic activities (β1, β2, β5)

of the proteasome as previously described.[13] Bortezomib (BTZ) (LC Laboratories, Woburn, MA) and the immunoproteasome inhibitor ONX-0914 (UBP Bio, Aurora, CO) were used as controls. Purified 20*S* constitutive proteasome from human erythrocytes or immunoproteasome from human peripheral blood mononuclear cells (PBMCs) (Boston Biochem, Cambridge, MA) and luminogenic substrates Z-LRR-Glo, Z-nLPnLD-Glo, and Suc-LLVY-Glo (Promega, Fitchburg, WI) specific for the β1, β2, and β5 (also referred to as T-L, C-L, and CT-L) catalytic subunit activities, respectively, were used. Briefly, 2.2 ng/µl of constitutive and immunoproteosome were incubated with increasing concentration of proteasome inhibitor (0 to 10 µM) in 10 mM HEPES, pH 7.3, for two hours at 37 ºC. Equal volume of the appropriate luminogenic substrate was added to each reaction and luminescence was measured 10 minutes later using a Multi-Mode Synergy (Biotek, Inc., Winooski, VT) plate reader. Assays were done in triplicate (n=3). The Ki-50 values for each catalytic activity were determined for each of the inhibitors using Graphpad Prism 5 software (La Jolla, CA) and averaged using Microsoft Excel (Redmond, WA).

Cell Viability Assay. To determine the effect of the thiasyrbactins proteasome inhibitors on the viability of cancer cells, three different human neuroblastoma (NB) cell lines were used. BTZ was included as a control. SK-N-Be(2)c, SK-N-SH cells (ATCC, Manassas, VA) and MYCN2 cells (provided by Dr. Jason Shohet, Texas Children's Hospital)[34] were plated overnight in RPMI media containing 10% heat-inactivated fetal bovine serum (FBS) (Invitrogen, Carlsbad, CA, USA), supplemented with penicillin (100 U/ml) and streptomycin (100 μg/ml). Cells were cultured at 37 °C in a humidified atmosphere containing 5% CO2 and treated with 0.01, 0.1 and 1 μM proteasome inhibitor for 24 hours. Cell viability was determined using the Cell Titer 96 AQueous One Cell Proliferation Assay (Promega) reagent MTS by measuring absorbance at 490 nm using a Multi-Mode Synergy plate reader as previously described.[13] Assays were done in

duplicate with triplicate wells of treatment per experiment (n=6). Data were expressed as the average cell viability relative to untreated control cells using Microsoft Excel.

Author Contributions

M.C.P., C.-E. C., and A.S.B. designed the study. N.A.B. performed the chemical synthesis of NAM compounds. C.R.S and L.P.Y. performed the biological studies including the in vitro proteasome activity assay and cell viability assay. C. C. R. performed the computational analysis. The manuscript was written through contributions of all authors. All authors have given approval to the final version of the manuscript.

Declaration of interests

M.C.P., N.A.B., and A.S.B. are named inventors on a US Patent application concerning the thiasyrbactins.

Acknowledgments

Nicole A. (Mikulski) Bakas was supported by a US Department of Education Graduate Assistance in Areas of National Need fellowship (award #P200A120170). Lisette P. Yco and Chad R. Schultz were supported by MSU internal funds to A.S.B. We thank Dr. Jason Shohet (Texas Children's Hospital, Houston, TX, USA) for providing cell line MYCN2.

References and notes

1. Krahn, D.; Ottmann, C.; Kaiser, M. The chemistry and biology of syringolins, glidobactins and cepafungins (syrbactins). *Nat. Prod. Rep.* **2011**, *28*, 1854-67.

2. Barr, P.; Fisher, R.; Friedberg, J. The role of bortezomib in the treatment of lymphoma. *Cancer Invest.* **2007**, *25*, 766-75.

3. Sugumar, D.; Keller, J.; Vij, R. Targeted treatments for multiple myeloma: specific role of carfilzomib. *Pharmgenomics Pers Med*. **2015**, *8*, 23-33.

4. Torimoto, Y.; Shindo, M.; Ikuta, K.; Kohgo, Y. Current therapeutic strategies for multiple myeloma. *Int. J. Clin. Oncol*. **2015**, *20*, 423-30.

5. Groll, M.; Schellenberg, B.; Bachmann, A.S.; Archer, C.R.; Huber, R.; Powell, T.K.; Lindow, S.; Kaiser, M.; Dudler, R. A plant pathogen virulence factor inhibits the eukaryotic proteasome by a novel mechanism. *Nature* **2008**, *452*, 755-8.

6. Coleman, C. S.; Rocetes, J. P.; Park, D. J.; Wallick, C. J.; Warn-Cramer, B. J.; Michel, K.; Dudler, R.; Bachmann, A. S. Syringolin A, a new plant elicitor from the phytopathogenic bacterium *Pseudomonas syringae pv. syringae*, inhibits the proliferation of neuroblastoma and ovarian cancer cells and induces apoptosis. *Cell Prolif*. **2006**, *39*, 599-609.

7. Krysiak, J.; Breinbauer, R. Activity-based protein profiling for natural product target discovery in Sieber, S. A., Ed., *Top. Curr. Chem*. **2012**, *324*, Springer, Berlin pp 43-84.

8. Carmony, K. C.; Kim, K. B. Activity-based imaging probes of the proteasome. *Cell Biochem. Biophys*. **2013**, *67*, 91-101.

9. Chiba, T.; Hosono, H.; Nakagawa, K.; Asaka, M.; Takeda, H.; Matsuda, A.; Ichikawa, S. Total synthesis of syringolin A and improvement of its biological activity. *Angew. Chem. Int. Ed*. **2014**, *53*, 4836–4839.

10. Clerc, J.; Groll, M.; Illich, D. J.; Bachmann, A. S.; Huber, R.; Schellenberg, B.; Dudler, R.; Kaiser, M. Synthetic and structural studies on syringolin A and B reveal critical determinants of selectivity and potency of proteasome inhibition. *Proc. Natl. Acad. Sci. USA* **2009**, *106*, 6507-12.

11. Clerc, J.; Li, N.; Krahn, D.; Groll, M.; Bachmann, A. S.; Florea, B. I.; Overkleeft, H. S.; Kaiser, M. The natural product hybrid of syringolin A and glidobactin A synergizes proteasome inhibition potency with subsite selectivity. *Chem. Commun.* **2011**, *47*, 385-7.

12. Clerc, J.; Schellenberg, B.; Groll, M.; Bachmann, A. S.; Huber, R.; Dudler, R.; Kaiser, M. Convergent synthesis and biological evaluation of syringolin A and derivatives as eukaryotic 20S proteasome inhibitors. *Eur. J. Org. Chem.* **2010**, 3991-4003.

13. Ibarra-Rivera, T. R.; Opoku-Ansah, J.; Ambadi, S.; Bachmann, A. S.; Pirrung, M. C. Synthesis and cytotoxicity of syringolin B-based proteasome inhibitors. *Tetrahedron* **2011**, *67*, 9950-6.

14. Bachmann, A. S.; Opoku-Ansah, J.; Ibarra-Rivera, T. R.; Yco, L. P.; Ambadi, S.; Roberts, C. C.; Chang, C. A.; Pirrung, M. C. The syrbactin structural analog TIR-199 blocks proteasome activity and induces tumor cell death. *J. Biol. Chem.* **2016**, *291*, 8350-62.

15. Oka, M.; Yaginuma, K.; Numata, K.; Konishi, M.; Oki, T.; Kawaguchi, H. Glidobactins A, B and C, new antitumor antibiotics. II. Structure elucidation. *J. Antibiot.* **1988**, *41*, 1338-50.

16. Lovering, F.; Bikker, J.; Humblet, C. Escape from flatland: increasing saturation as an approach to improving clinical success. *J. Med. Chem.* **2009**, *52*, 6752-6.

17. Lovering, F. Escape from Flatland 2: complexity and promiscuity. *Med. Chem. Commun.* **2013**, *4*, 515-519.

18. Ishikawa, M.; Hashimoto, Y. Improvement in aqueous solubility in small molecule drug discovery programs by disruption of molecular planarity and symmetry. *J. Med. Chem.* **2011**, *54*, 1539-54.

19. Lagorce, D.; Sperandio, O.; Baell, J. B.; Miteva, M. A.; Villoutreix, B. O. FAF-Drugs3: a web server for compound property calculation and chemical library design. *Nucleic Acids Res*. **2015**, 43, (Web Server issue) W200-W207.

20. Lusci, A.; Pollastri, G.; Baldi, P. Deep architectures and deep learning in chemoinformatics: The prediction of aqueous solubility for drug-like molecules. *J. Chem. Inf. Model*. **2013**, 53, 1563-1575.

21. Schauer, D.J.; Helquist, P. Mild zinc-promoted Horner-Wadsworth-Emmons reactions of diprotic phosphonate reagents. *Synthesis* **2006**, 3654-3660.

22. Fraser, R. R.; Schuber, F. J.; Wigfield, Y. Y. Conformational preference of an α-sulfinyl carbanion. *J. Am. Chem. Soc*. **1972**, *94*, 8795–8799.

23. Levin, N.; Spencer, A.; Harrison, S. J.; Chauhan, D.; Burrows, FJ.; Anderson, KC.; Reich, SD.; Richardson, PG.; Trikha, M. Marizomib irreversibly inhibits proteasome to overcome compensatory hyperactivation in multiple myeloma and solid tumour patients. *Br. J. Haematol*. **2016**, 174, 711-720.

24. Kraus, J.; Kraus, M.; Liu, N.; Besse, L.; Bader, J.; Geurink, P. P.; de Bruin, G.; Kisselev, A. F.; Overkleeft, H.; Driessen, C. The novel β2-selective proteasome inhibitor LU-102 decreases phosphorylation of I kappa B and induces highly synergistic cytotoxicity in combination with ibrutinib in multiple myeloma cells. *Cancer Chemother. Pharmacol*. **2015**, 76, 383-96.

25. Kraus, M.; Bader, J.; Geurink, PP.; Weyburne, ES.; Mirabella, AC.; Silzle, T.; Shabaneh, TB.; van der Linden, WA.; de Bruin, G.; Haile, SR.; van Rooden, E.; Appenzeller, C.; Li, N.; Kisselev, A. F.; Overkleeft, H.; Driessen, C. The novel β2-selective proteasome inhibitor LU-

102 synergizes with bortezomib and carfilzomib to overcome proteasome inhibitor resistance of myeloma cells. *Haematologica* **2015**, *100*, 1350-60.

26. Koroleva, O. N.; Pham, T. H.; Bouvier, D.; Dufau, L.; Qin, L.; Reboud-Ravaux, M.; Ivanov, A. A.; Zhuze, A. L.; Gromova, E. S.; Bouvier-Durand, M. Bisbenzimidazole derivatives as potent inhibitors of the trypsin-like sites of the immunoproteasome core particle. *Biochimie* **2015**, *108*, 94-100.

27. Mirabella, A. C.; Pletnev, A. A.; Downey, S. L.; Florea, B. I.; Shabaneh, T. B.; Britton, M.; Verdoes, M.; Filippov, D. V.; Overkleeft, H. S.; Kisselev A. F. Specific cell-permeable inhibitor of proteasome trypsin-like sites selectively sensitizes myeloma cells to bortezomib and carfilzomib. *Chem. Biol.* **2011**, *18*, 608-18.

28. Kaur, G.; Batra, S. Emerging role of immunoproteasomes in pathophysiology. *Immunol. Cell Biol.* **2016**, *94*, 812-820.

29. Groettrup, M.; Kirk, C. J.; Basler, M. Proteasomes in immune cells: more than peptide producers? *Nat. Rev. Immunol.* **2010**, *10*, 73-78.

30. Martinon, F.; Aksentijevich, I. New players driving inflammation in monogenic autoinflammatory diseases. *Nat. Rev. Rheumatol.* **2015**, *11*, 11-20.

31. Kuhn, D. J.; Hunsucker, S. A.; Chen, Q.; Voorhees, P. M.; Orlowski, M.; Orlowski, R. Z. Targeted inhibition of the immunoproteasome is a potent strategy against models of multiple myeloma that overcomes resistance to conventional drugs and nonspecific proteasome inhibitors. *Blood* **2009**, *113*, 4667-76.

32. Miller, Z.; Lee, W.; Kim, K. B. The immunoproteasome as a therapeutic target for hematological malignancies. *Curr. Cancer Drug Targets* **2014**, *14*, 537-48.

33. Baell, J. B.; Holloway, G. A. New substructure filters for removal of pan assay interference compounds (PAINS) from screening libraries and for their exclusion in bioassays. *J. Med. Chem.* **2010**, *53*, 2719-2740.

34. Slack, A.; Chen, Z.; Tonelli, R.; Pule, M.; Hunt, L.; Pession, A.; Shohet, J. M. The p53 regulatory gene MDM2 is a direct transcriptional target of MYCN in neuroblastoma. *Proc. Natl. Acad. Sci. USA* **2005**, *102*, 731-736.

Supplementary Materials. Comparison of modeled and calculated dihedral angles in **12**. Effect of thiasyrbactins on *in vitro* proteasome activity. NMR spectra of new compounds (34 pages total). This material is available free of charge via the Internet.

Graphical Abstract

To create your abstract, type over the instructions in the template box below.
Fonts or abstract dimensions should not be changed or alter

Immunoproteasome Inhibition and Bioactivity of Thiasyrbactins

Leave this area blank for abstract info.

Nicole A. Bakas,[1] Chad R. Schultz,[2] Lisette P. Yco,[2] Christopher C. Roberts,[1] Chia-en A. Chang,[1] André S. Bachmann,*[2] and Michael C. Pirrung*[1,3]

[1]Department of Chemistry, University of California, Riverside, CA 92521, USA. [2]Department of Pediatrics and Human Development, College of Human Medicine, Michigan State University, Grand Rapids, MI 49503, USA. [3]Department of Pharmaceutical Sciences, University of California, Irvine, CA 92697 USA.